Streak camera crosstalk reduction using a multiple delay optical fiber bundle

Anthony Tsikouras[1], Jin Ning[2], Sandy Ng[3], Richard Berman[3], David W. Andrews[4], and Qiyin Fang[1,2,*]

[1]*Department of Engineering Physics, McMaster University, 1280 Main Street West, Hamilton, Ontario L8S 4L7, Canada*

[2]*Department of Biomedical Engineering, McMaster University, 1280 Main Street West, Hamilton, Ontario L8S 4L7, Canada*

[3]*Spectral Applied Research, 9078 Leslie Street Unit 11, Richmond Hill, Ontario L4B 3L8, Canada*

[4]*Department of Biochemistry and Biomedical Sciences, McMaster University, 1280 Main Street West, Hamilton, Ontario L8S 4L7, Canada*

**Corresponding author: qiyin.fang@mcmaster.ca*

Received August 25, 2011; revised November 28, 2011; accepted November 28, 2011; posted November 30, 2011 (Doc. ID 153338); published January 13, 2012

The streak camera is one of the fastest photodetection systems, while its capability of multiplexing is particularly attractive to many applications requiring parallel data acquisition. The degree of multiplexing in a streak camera is limited by the crosstalk between input channels. We developed a technique that introducing a fixed time delay between adjacent fiber channels in a customized two-dimensional to one-dimensional fiber array to significantly reduce crosstalk both at the sample plane and at the input of a streak camera. A prototype system has been developed that supports 100 input channels, and its performance in fluorescence microscopy is demonstrated.

OCIS codes: 180.2520, 060.4230.

A streak camera is one of the fastest time-domain photodetection systems with picoseconds resolution [1–3], which is achieved by using a time-varying voltage to deflect photoelectrons perpendicular to their direction of travel. The time of photoelectron generation therefore correlates to spatial position on a readout camera.

Over the past two decades, several groups have developed streak camera based fluorescence lifetime imaging microscopy (FLIM) techniques [3–8], which measure fluorescence lifetime in addition to intensity [9–13]. For example, Krishnan *et al.* developed a multiphoton FLIM system with both high temporal resolution (from the streak camera) and spatial resolution (from the scanning multiphoton illumination) [6,7]. In this design, a single excitation point is raster scanned across the field of view to generate a two-dimensional (2D) lifetime image.

Similar to an imaging spectrograph, a streak camera supports multiple input channels, which makes it inherently suited for high-throughput applications such as FLIM. Qu *et al.* [8] and Shao *et al.* [14] used a microlens array to divide a laser beam into a 4×4 array of foci, and also a special streak camera input consisting of a matching pinhole array. A prism was used after the pinhole input, resulting in a 4×4 array of streak images combined with spectral information. This approach led to a substantial improvement of throughput by multiplexing, but it required a special wide photocathode [8] and further multiplexing was limited by the photocathode's spatial resolution [15]. The multiplexing ability is limited by crosstalk between adjacent input channels, which not only reduces image quality but also hinders the accurate estimation of time-domain data (e.g., lifetime). Instead of generating a 2D array at the input of a streak camera, we developed a 2D to one-dimensional (1D) fiber array that transfers the image of a 2D array of spots on the sample to a linear array entering a conventional streak camera with a slit photocathode. Crosstalk between channels at the sample plane on the 2D end is reduced by using a large pitch between individual channels. Throughput improvement may be realized by increasing the number of fibers in the array, which is limited by the spatial resolution of the photocathode and crosstalk between adjacent fiber inputs at the 1D end. (Details of this design will be reported elsewhere.)

Besides spatial separation, short pulses/decays may be separated in time, by varying the optical path length to introduce a delay in the time domain [16]. In this report, we present a novel fiber bundle design that can significantly reduce crosstalk at the 1D end of the streak camera input by introducing a fixed optical path length difference between adjacent fibers. We demonstrate that this design significantly reduces crosstalk between adjacent fibers such that it enables a much greater degree of multiplexing at the streak camera input. This design is applicable for not only FLIM but other multichannel applications using a streak camera.

Figure 1 shows the schematic of the experimental setup. Two microlenslet arrays (500 μm center-to-center pitch, square microlenses, SUSS MicroOptics, Neuchâtel, Switzerland) are used to generate arrays of excitation

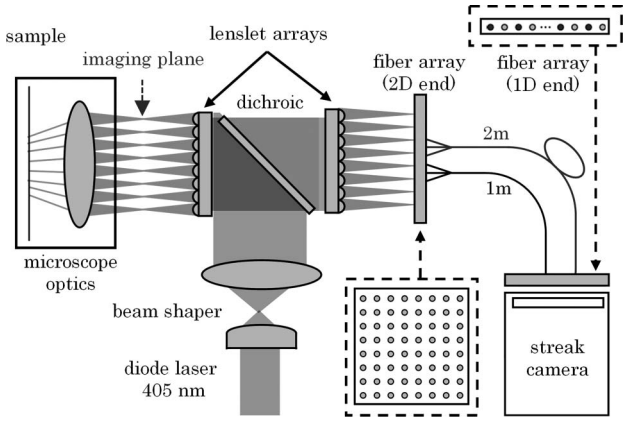

Fig. 1. Instrument setup for multiple delay optical fiber array streak imaging.

foci on the sample and focus the fluorescence emission to the fiber array. A diode laser (3 mW, 60 ps LDH-P-C-440M, PicoQuant, Berlin, Germany) provides pulsed excitation at 440 nm, which goes through the first lenslet array to generate a 10×10 array of foci. A 445 nm dichroic filter (Di01-R442-25 × 36, Semrock, Rochester, New York) reflects the beams to the side imaging port of an inverted fluorescence microscope (Axiovert 200, Carl Zeiss, Oberkochen, Germany). Fluorescence emission from the sample is relayed back through the two lenslet arrays and an emission filter (FF01-542/27-25, Semrock), then focused onto the 2D end of a customized 2D–1D fiber array (0.11 NA, fused silica, $n = 1.44$, 50 μm diameter core, 50 μm cladding). At the 1D end of the fiber array, the fibers are arranged into a linear 1×100 array and coupled to the input slit of a streak camera (SC-10, Optronis, Kehl, Germany). In the fiber array, adjacent fibers are of alternating lengths of 1 and 2 m, which leads to a temporal separation of 4.8 ns. This temporal separation is translated into a spatial separation of 4.8 mm when sweeping at 1 ns/mm. FLIM acquisition is achieved by raster scanning the sample so that the 2D foci array covers the full frame. A lookup table correlating the 2D foci array to the 1D array on the streak camera readout is used to reconstruct the final FLIM image.

The overall system temporal response is limited by a number of factors, including the laser pulse width (60 ps), the fiber modal dispersion (15–30 ps), and the fiber core size (50 μm), which translates to a 50 ps spot at the streak camera readout. The impulse response of the system is measured to be 126 ps FWHM.

To demonstrate the crosstalk reduction using the alternating fiber delay lines, Coumarin 6 (546283, Sigma-Aldrich, St. Louis, Missouri) dissolved in ethanol solution (5 μM) is measured to form a uniform distributed image using the sweep on and sweep off modes of the streak camera. The sweep on mode is the normal operating mode, where a time-varying ramp voltage is applied in the horizontal (temporal) direction. As shown in Fig. 2(b), fluorescence decay from each fiber becomes a streak on the readout camera. In this case, the difference in fiber lengths results in a right shift of 4.8 mm for longer fibers, which are spatially separated from streaks from the adjacent shorter fibers. As shown in Fig. 2, each of the streaks is visibly separate with low crosstalk between adjacent channels.

To quantify the reduction in crosstalk achieved using alternating 1 and 2 m fibers, the extent of crosstalk when the fiber delay is not present was simulated by acquiring images using the sweep off mode. In this mode, there is no time-dependent deflection of electrons, such that all photoelectrons reach the readout camera at the same time-axis location. As a result, the time delay between adjacent fibers does not lead to spatial separation on the readout camera, which is similar to the crosstalk between two adjacent streaks when the time delay is not present. As shown in Fig. 2(c), the crosstalk between adjacent spots is obvious when the streak camera is operated in the sweep off mode.

To compare the crosstalk between the two modes quantitatively, intensity profiles of the spots in Fig. 2(a) and the streaks in Fig. 2(b) were calculated with the background noise subtracted. The crosstalk between

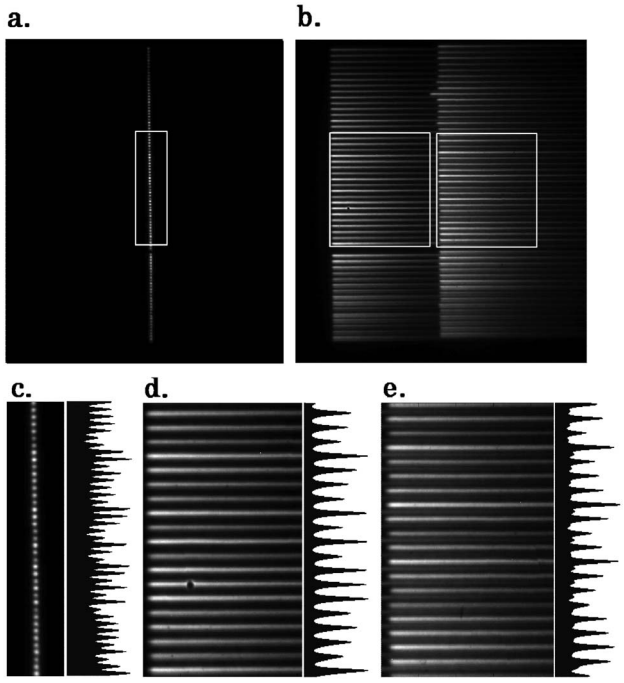

Fig. 2. Streak images of fiber array inputs, with corresponding intensity profiles. (a) Fiber array imaged at the sweep off mode, (b) fiber array imaged at the sweep on mode. The left and right columns of streaks are from the 1 and 2 m fibers, respectively. (c) Magnified view of spots in the sweep off mode with corresponding intensity profile, (d), (e) magnified views of the sweep off mode and the corresponding intensity profiles.

adjacent channels was defined by the ratio of the valley between two spots to the average of the two adjacent peaks. The crosstalk in sweep off mode, which simulates a fiber array without alternating fiber lengths, was $52 \pm 11\%$. The crosstalk in sweep on mode was $19 \pm 4\%$ and $33 \pm 11\%$ for 1 m fibers and 2 m fibers, respectively. The 2 m fibers have significantly more crosstalk with the addition of the residual decay from the 1 m streaks, which may be removed using incomplete decay algorithms [17–18]. The lifetime of the Coumarin 6 was 2.58 ± 0.04 ns when fitted to a multiexponential decay. It is in good agreement with literature reported values [19].

Figure 3 shows steady-state fluorescence images of fixed *Convallaria* specimens (*Convallaria majalis* fixed sample, Leica, Wetzlar, Germany) using the fiber array multiplexing method presented. The *Convallaria* sample is stained with safranin (530 nm, 590 nm) and fast green (620 nm, 660 nm) [20]. The sample was scanned using an *X*-*Y* stage with 40 steps and a 20× objective. The resulting image resolution is 1.3 μm, but the resolution can be improved to the objective limit of 0.6 μm by increasing the number of steps taken by the *X*-*Y* stage. Figure 3(a) shows the fluorescence image acquired in the sweep off mode, simulating the situation in which there is no fiber delay present.

The images were reconstructed from the 1600 streak images. Furthermore, a normalization factor was applied to each channel to correct its intensity variations. The normalization table was obtained by each channel's intensity measurement when imaging a uniform paper fluorescence standard.

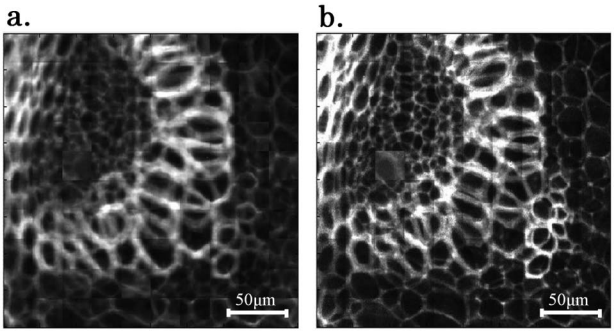

Fig. 3. Reconstructed fluorescence intensity images of fixed *Convallaria* specimens imaged (a) without sweeping and (b) with sweeping. When the streak camera is not sweeping (a), the fiber delay between adjacent fibers is not present and the image is reconstructed from steady-state acquisitions such as in Fig. 2(c). When the streak camera is sweeping (b), the image is reconstructed from time-resolved acquisitions such as in Figs. 2(d)–(e).

To acquire the images shown in Fig. 3, 0.5 s integration was required for each step, depending on sweep mode. This leads to over 800 s to acquire a full FLIM image. It should be noted that the current FLIM setup is optimized not for high speed but for the demonstration of the performance of crosstalk reduction. For example, the diode laser pulse energy is 75 pJ/pulse, which is shared by over 100 foci. The acquisition time in this setup is also limited by the 4 MHz repetition rate of the streak camera, where the laser can operate at 40 MHz. A higher intensity laser and high repetition synchroscan sweeping module can significantly improve acquisition speed.

Figure 3(b) shows the time-integrated fluorescence image of the same sample region in the sweep on mode demonstrating the reduced crosstalk. Although the sweep off mode image [Fig. 3(a)] shows better signal intensity, the sweep on image [Fig. 3(b)] shows significantly improved contrast from lower crosstalk. This is especially apparent in the low-signal regions of the image, where crosstalk from an adjacent fiber would be especially detrimental.

The lifetime of most fluorescent probes used in FLIM are shorter than 4 ns. By introducing a 4.8 ns delay, lifetime estimation based on the intensity decay of the shorter fiber is minimally affected by the adjacent longer fibers. Nonetheless, different delay times can be introduced by using fibers of different lengths. A time-domain signal measured from the longer fibers only suffers from the residual decay (>4.8 ns) from the shorter fibers. This is similar to the incomplete decay effect commonly seen with high repetition rate laser excitation and may be corrected mathematically [17,18]. Depending on the lifetime being studied, signal multiplexing may be increased further by introducing more groups with different delays. In addition to lifetime, the time delay is also limited by the overall width of the time window on the streak camera (20 ns in our case).

Because of the length limitation of this short communication, fluorescence lifetime imaging results as well as a detailed description of the FLIM system setup will be reported elsewhere. It is, however, important to confirm that the delayed fibers are able to measure the same lifetime decays as the nondelayed fibers.

In summary, alternating the length of adjacent fibers significantly reduces crosstalk between adjacent fiber channels and thereby increases the degree of multiplexing possible when using a streak camera to measure multiple input channels simultaneously. This technique is expected to be particularly useful both for live cell imaging and for high-throughput automated imaging as is used in drug discovery systems, where the speed at which a FLIM image is acquired is a major hurdle.

The authors would like to thank P. Sinclair for his assistance in the FLIM system design. This project is supported by funding from the Canadian Institutes of Health Research [161934 (Q. F. & D. W. A.); FRN 10490 (D. W. A.)], the Ontario Centres of Excellence (Q. F. & D. W. A.), the Canadian Foundation of Innovation/Ontario Ministry of Research and Innovation (Q. F. & D. W. A.), and the Natural Sciences & Engineering Research Council. (D. W. A. holds the Canada Research Chair in Membrane Biogenesis; Q. F. holds the Canada Research Chair in Biophotonics).

References

1. A. J. Campillo and S. L. Shapiro, IEEE J. Quantum Electron. **19**, 585 (1983).
2. M. Nisoli and G. Sansone, Prog. Quantum Electron. **33**, 17 (2009).
3. J. Mizeret, T. Stepinac, M. Hansroul, A. Studzinski, H. van den Bergh, and G. Wagnieres, Rev. Sci. Instrum. **70**, 4689 (1999).
4. C. Biskup, T. Zimmer, and K. Benndorf, Nat. Biotech. **22**, 220 (2004).
5. A. Kusumi, A. Tsuji, M. Murata, Y. Sako, A. C. Yoshizawa, S. Kagiwada, T. Hayakawa, and S. Ohnishi, Biochemistry **30**, 6517 (1991).
6. R. V. Krishnan, A. Masuda, V. E. Centonze, and B. Herman, J. Biomed. Opt. **8**, 362 (2003).
7. R. V. Krishnan, H. Saitoh, H. Terada, V. E. Centonze, and B. Herman, Rev. Sci. Instrum. **74**, 2714 (2003).
8. J. Qu, L. Liu, D. Chen, Z. Lin, G. Xu, B. Guo, and H. Niu, Opt. Lett. **31**, 368 (2006).
9. I. Bugiel, K. König, and H. Wabnitz, Lasers Life Sci. **3**, 47 (1989).
10. X. F. Wang, T. Uchida, and S. Minami, Appl. Spectrosc. **43**, 840 (1989).
11. Y. Fu and J. R. Lakowicz, Anal. Chem. **78**, 6238 (2006).
12. Y. Chen and A. Periasamy, Microsc. Res. Tech. **63**, 72 (2004).
13. T. French, P. T. C. So, D. J. Weaver, T. C. Sampaio, E. Gratton, E. W. Voss, and J. Carrero, J. Microsc. **185**, 339 (1997).
14. Y. Shao, J. Qu, H. Li, J. Qi, G. Xu, and H. Niu, Appl. Phys. B **99**, 633 (2010).
15. M. Clampin and F. Paresce, Rev. Sci. Instrum. **60**, 1092 (1989).
16. Y. Yuan, T. Papaioannou, and Q. Fang, Opt. Lett. **33**, 791 (2008).
17. R. W. K. Leung, S. A. Yeh, and Q. Fang, Biomed. Opt. Express **2**, 2517 (2011).
18. Y. Sakai and S. Hirayama J. Lumin. **39**, 145 (1988).
19. Y. Sun, R. N. Day, and A. Periasamy, Nat. Protoc. **6**, 1324 (2011).
20. J. H. Frank, A. D. Elder, J. Swartling, A. R. Venkitaraman, A. D. Jeyasekharan, and C. F. Kaminski, J. Microsc. **227**, 203 (2007).